PROCEEDINGS, 50th Workshop on Geothermal Reservoir Engineering
Stanford University, Stanford, California, February 10-12, 2025
SGP-TR-229

# High-Temperature Triaxial Direct Shear Testing for Utah FORGE

Bijay KC*[1]; Luke P. Frash*[1]; Uwaila C. Iyare[1]; Wenfeng Li[1]; Yerkezhan Madenova[1,2]; Megan Smith[3]; Kayla Kroll[3]

[1] Earth and Environmental Sciences Division, Los Alamos National Laboratory, Los Alamos, NM, USA

[2] University of Wisconsin – Madison, Madison, WI, USA

[3] Atmospheric, Earth and Energy Division, Lawrence Livermore National Laboratory, Lawrence, CA, USA

* bkc@lanl.gov; lfrash@lanl.gov

**Keywords:** Slickensides, TDS, Shear Strength, Dilation, Fracture, Permeability, Shear

## ABSTRACT

Measurements of the coupled thermo-hydro-mechanical-chemical (THMC) properties of rock fractures are sparse, and even more so at high-temperature. The Utah Frontier Observatory for Research in Geothermal Energy (FORGE) has a reservoir temperature near 200 °C, hydrostatic pressure exceeding 20 MPa, and minimum principal stress exceeding 35 MPa. Here, we present the results of our laboratory experiments to measure the THMC properties of shear fractures that are created and slip-stimulated at FORGE site conditions. Our rock samples are granite and gneiss specimens taken from well 16A(78)-32. Our methodology is triaxial direct-shear with high-temperature. Injected fluids mimic the chemistry of a previously planned injectate, sourced from a nearby golf course. Using intact samples, our results provide measurements for the shear strength, dilation, permeability, hydraulic aperture, stress-dependent aperture, and effluent chemistry. This information provides data for modeling the FORGE site, and for other sites having a similar geologic setting.

## 1. INTRODUCTION

Geothermal energy is a promising renewable energy source that can provide clean base load energy for electricity and heat. U.S. Department of Energy reports geothermal energy could provide 60 GWe by 2050 considering technological improvements over time (Augustine et al., 2019). Enhanced Geothermal System (EGS) is key to unlocking this potential. EGS is characterized with hot dry rock that requires stimulation to enhance permeability to circulate water at an economic rate for heat extraction (Brown et al., 2012; Tester et al., 2006). As such, understanding the fracture response to coupled thermo-hydro-mechanical-chemical (THMC) processes remains a key research topic for development of economic EGS (Frash et al., 2024; Dobson et al., 2021; Kneafsey et al., 2021).

The Frontier Observatory for Research in Geothermal Energy (FORGE) is the Department of Energy's (DOE) subsurface laboratory to research and advance EGS development. The goal of the FORGE project is to develop, test, and accelerate the breakthroughs in technologies required for creating, sustaining, and monitoring EGS reservoirs for commercializing EGS resources (Moore et al., 2020; 2023). The FORGE site is located near Milford, Utah on the western flank of Mineral Mountains. The nearby area around the FORGE site has been home to numerous geothermal power plants, for example PacifiCorp Energy's Blundell geothermal plant, Cyrq Energy's plant, and Fervo Energy's Cape Station project (Allis and Larsen, 2012; Cyrq Energy, 2025; Norbeck et al., 2024). In January 2021, a highly deviated injection well 16A(78)-32 was completed, which was later hydraulically stimulated to create an EGS reservoir. Another well, 16B(78)-32, was drilled into the stimulated fracture network to serve as a production well, forming a doublet system with spacing of ~ 100 m. The reservoir depth and temperature at FORGE site are nominally 2600 m and 200 °C (Jones et al., 2024; McLennan et al. 2023; Moore et al., 2020 & 2023).

This study characterizes the thermal, hydraulic, and mechanical (TMH) coupled processes related to the stimulation and flow of fluid through shear induced fractures in the EGS reservoir at the FORGE site. To achieve our goals, we employed a Triaxial Direct Shear (TDS) procedure to create a shear fracture at in-situ conditions and measure the intact and fracture permeability, while also assessing the impact of coupled THM processes on the fracture permeability. Results from this study reveal insights into the potential of enhancing reservoir permeability through shear stimulation and quantify fractures properties at in-situ conditions, including strength, frictional properties, dilation tendencies, and fracture compressibility, which are each input parameters for field-scale reservoir simulation.

## 2. MATERIALS AND METHODS

### 2.1 ROCK SPECIMENS AND INJECTATE FLUID

We prepared cylindrical specimens with 38.1 mm (1.5 inch) diameter and 38.1 mm length from subsurface cores retrieved from well 16A(78)-32 at the FORGE site. The key information of the specimens along with the experimental conditions are summarized in Table 1. The specimens were primarily granite, gneiss, and granodiorite. The specimens were foliated (FS09) and featured small-cracks (FS02) (Figure 1). For these specimens, we orient the fabric of the foliation or cracks to be parallel to shear direction with an intention to induce the shear fracture along these weak planes. This is a logical approach as shearing of weak features is most prevalent in-situ during EGS stimulation. The injectate fluid was synthesized in the laboratory to mimic the chemistry of the water sourced from a nearby golf course, which was a previously planned injectate fluid. The fluid is a 0.5 mM solution consisting of 3.2 mg/L KCl, 47.7 mg/L $CaCl_2.2H_2O$, 33.5 mg/L $MgCl_2.6H_2O$, 53.2 mg/L $Na_2SO_4$, and 0.032 mg/L $NaHCO_3$ added to deionized water.

Table 1. Properties of rock specimens from 16A(78)-32 with experimental conditions.

| Specimen ID | Rock Type | Retrieval Depth (m)* | Density ($kg/m^3$) | Test Temperature (°C) | Confining Stress (MPa) | Pore Pressure (MPa) |
|---|---|---|---|---|---|---|
| FS02 | Granitic | 3345 | 2647.5 | 23 ± 3 | 36.1 | 22 |
| FS09 | Gneissic | 3339 | 2788.4 | 195 ± 15 | 36.1 | 22 |

* The retrieval depth is the measured depth. The true vertical depth of the specimens is 2200 m.

### 2.2 SAMPLE PREPARATION

Our sample preparation technique for the high temperature triaxial direct shear test builds upon our previous failures and successes (Frash et al., 2024; Iyare et al., 2024). We start by wrapping the cylindrical specimens inside a heat shrink Teflon to cover the specimen from end to end. The Teflon will ensure that the flow is contained within the fracture after shearing. Then we put the Teflon wrapped specimen inside the Viton sleeve. The Viton sleeve isolates the specimen from the confining fluid. Due to its elasticity, the Viton sleeve can ensure the complete isolation even at larger fracture displacements under high temperatures. In our previous experiments, we observed the sharp edges of the fracture cut through the Viton sleeve at high pressure and temperature condition compromising the experiment. So, we inserted two metal shims between the Teflon and Viton at the pre-determined location where the fracture would be created. Then, we attached the two opposing L-shaped platens on both ends of the specimen using steel wire tourniquets. We used temperature resistant silicone rubber to fill the gap on the platens. Due to the L-shape of the platen, axial force applied on the sample induces direct shear stress along targeted plane on the specimen. Finally, we mount a pair of axial Linear Variable Displacement Transducers (LVDT) and one radial LVDT at the center to measure the deformation during the experiment. The entire sample assembly was then placed on the triaxial cell base and vacuum tested to confirm the seal of the assembly and prevent any leakage during the test (Figure 1).

### 2.3 MIMICKING IN-SITU CONDITIONS

To mimic the in-situ stress condition in our experiments, we used the stress estimates for FORGE by Xing et al., (2020), which reports the total maximum and minimum principal stress of 63.4 MPa and 32.5 MPa, respectively. It should be noted that we used the stress estimates from 2020 to cross-compare our previous experimental results even though the in-situ stress estimates at FORGE are updated regularly. Readers are advised to read the most recent literature for the updated stress regime at FORGE. We assumed a slip plane at 20° angle with respect to the maximum principal stress to determine the total normal stress on the fracture to be 36.1 MPa, which is the confining pressure for our experiments. We estimated the pore pressure for the experiments as 22 MPa, which is the hydrostatic pressure at depth of 2200 m from where the specimens were retrieved. The temperature conditions for our experiments were 195 ± 15 °C based on the in-situ conditions and the limits of our heater system. We also conducted one experiment at room temperature to evaluate the impact of temperature on the fracture flow.

### 2.4 EXPERIMENTAL PROCEDURE

The unique feature of the triaxial direct shear procedure is its ability to measure the intact rock properties, then shear-fracture the rock and characterize the transport through the fractured rock, all under in-situ conditions without the necessity of artificially inducing the fracture. This method introduces fractures that are representative of fractures in field conditions compared to the most common methods that would use saw-cut or artificially fractured specimens. Each TDS platens consists of two fluid ports, one for the flow line and other for the static pressures for precise measurements of differential pore pressure across the sample. The intel and outlet pressure and flow through the specimen was controlled using syringe pumps. The redundancy in pressure measurement and flow measurement allows for the instantaneous assessment of the permeability and its uncertainty. The general procedures followed to perform the experiments in this study are:

(1) Pre-confinement: Set-up the specimen prepared in subsection 2.2 on the triaxial cell base and vacuum test to confirm seal of the assembly. Fill the cell with high temperature silicone oil, i.e. confining fluid.
(2) Heating: Start heating the sample by activating the heater on the triaxial cell to gradually increase the temperature of the confining fluid inside the cell. Confining pressure of 5 MPa was maintained during the heating process to prevent the steam pressure from fracturing the rock sample when temperature is above 90 °C. Heating rate was maintained at 0.75 °C/min until the target temperature of 195 °C was reached then the system was allowed to equilibrate for 2 hours.
(3) In-situ confinement: The confining pressure was increased to the target value of 36.1 MPa, and the pore pressure to 22 MPa.
(4) Intact rock permeability: We measured the intact rock permeability at in-situ conditions by injecting golf course water from top of the specimen.
(5) Fracturing and incremental shear: We sheared the sample by applying shear stress on the sample. The displacement rate of the axial piston was maintained at 0.002 mm/sec during all shearing stages. The fracture was displaced up to 2 mm to characterize the fracture permeability at different shear displacement levels.
(6) Confining stress cycle: Confining stress cycling (36.1 MPa – 24 MPa – 36.1 MPa – 48 MPa – 36.1 MPa) was performed to observe the hysteresis in the permeability due to change in normal stress.
(7) Mohr-Coulomb shear: The confining stress acting on the specimen was changed, and the fracture was sheared further by 0.3 mm steps to characterize the frictional properties of the fracture.
(8) Finally, the system was allowed to cool to ambient temperature before depressurizing and ending the experiment.

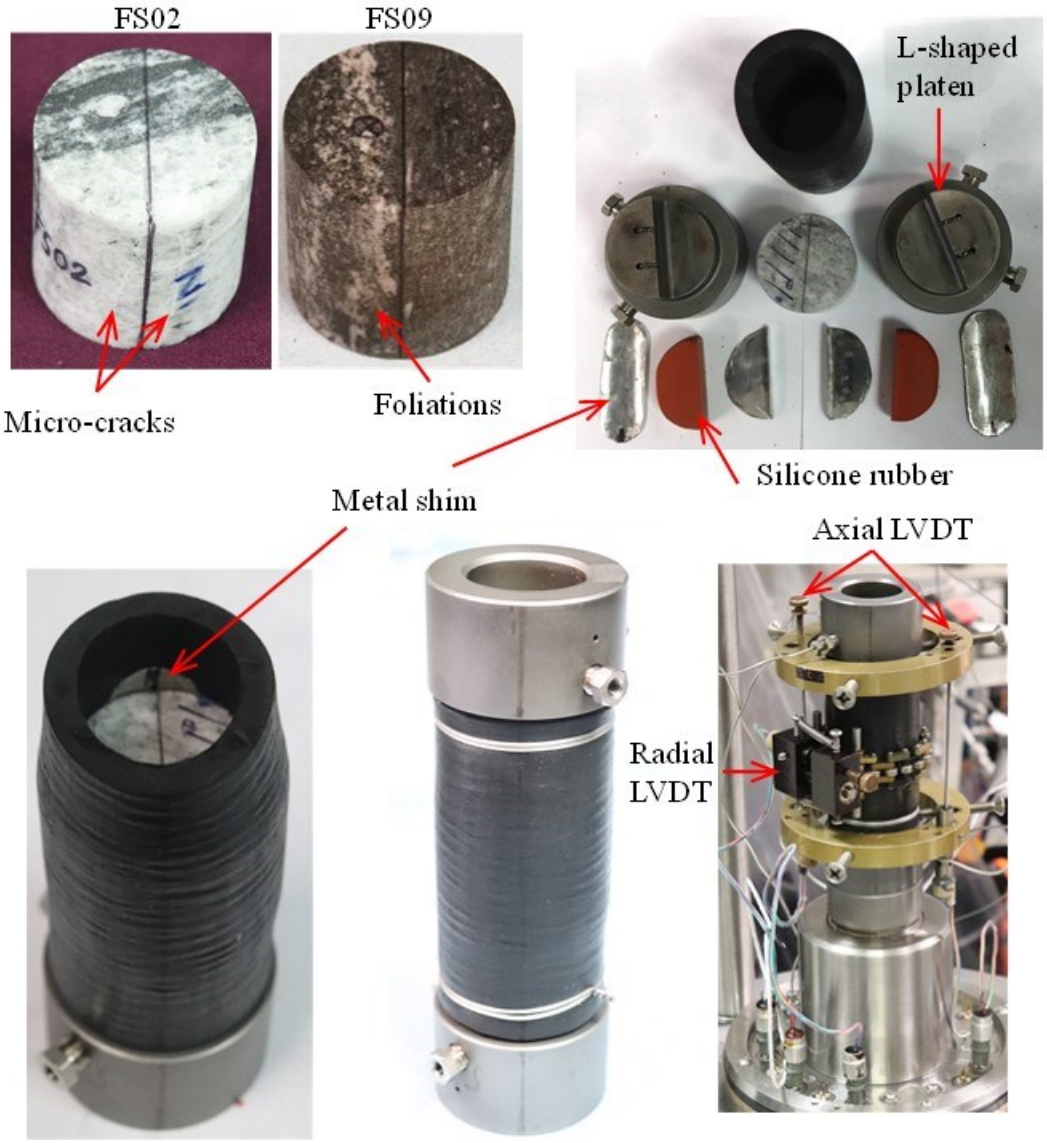


**Figure 1: Rock specimens and the sample assembly for triaxial direct-shear experiments. Two specimens, one granitic (FS02) and next gneissic (FS09) were prepared from the core retrieved from well 16A(78)-32 at FORGE. The specimen is placed between two L-shaped platens with high temperature silicone filler in such a way that the weak planes such as foliation is aligned parallel to the shear direction. Two stainless steel metal shims were inserted into the inner side of the Viton sleeve to prevent the sleeve failure at high temperature and pressure. Two axial LVDTs were mounted on opposite side of the fracture and one radial LVDT was mounted across the fracture.**

### 2.5 PERMEABILITY AND APERTURE MEASUREMENTS

In this study, we report the bulk specimen permeability calculated as:

$$k = \frac{4Q\mu L}{\pi D^2(P_i - P_o)} \tag{1}$$

where, $Q$ is the volumetric flow rate through, $\mu$ is the dynamic viscosity of water (0.15 cP at 200 °C; 0.9 cP at 23 °C), $L$ is length of the specimen, $D$ is diameter of the specimen, $P_i$ is inlet pressure, and $P_o$ is the outlet pressure. We measure the mechanical aperture ($b_d$) or fracture dilation in our experiment using radial LVDT data. It is important to distinguish the hydraulic aperture and mechanical aperture of the fracture. The mechanical aperture controls the fracture porosity, while the hydraulic aperture controls the flow through the fracture. The hydraulic aperture can be measured using the parallel plate model (Witherspoon et al., 1980) and is generally lower than the mechanical aperture because of the asperities, fracture roughness, and tortuosity (Li et al., 2021; Meng et al., 2022).

## 3. RESULTS AND DISCUSSIONS

### 3.1 INTACT AND FRACTURED PERMEABILITY

In this study, we present the results of TDS experiments on two specimens, namely FS02 and FS09. FS02 specimen was tested at room temperature and FS09 was tested at the in-situ temperature of 195 ± 15 °C. The time evolution of stresses, shear displacement, fracture dilation, and permeability evolution of the specimens are shown in Figure 2. The intact permeability of FS02 specimen was an order of magnitude higher than that of FS09 specimen, due to the presence of the small-cracks in FS02 specimen (Figure 1). Once the specimens are sheared, the bulk permeability of the specimen increased to tens to thousands of mD. This is 5 orders of magnitude increase in permeability in case of FS09 specimen and 4 orders of magnitude increase for FS02 specimen. The silicone rubber failure during the stress cycling stage (discussed in detail in sub-section 3.4) in FS09 specimen resulted in an erroneous permeability value, hence permeability values only up to shearing stage are shown in Figure 2.

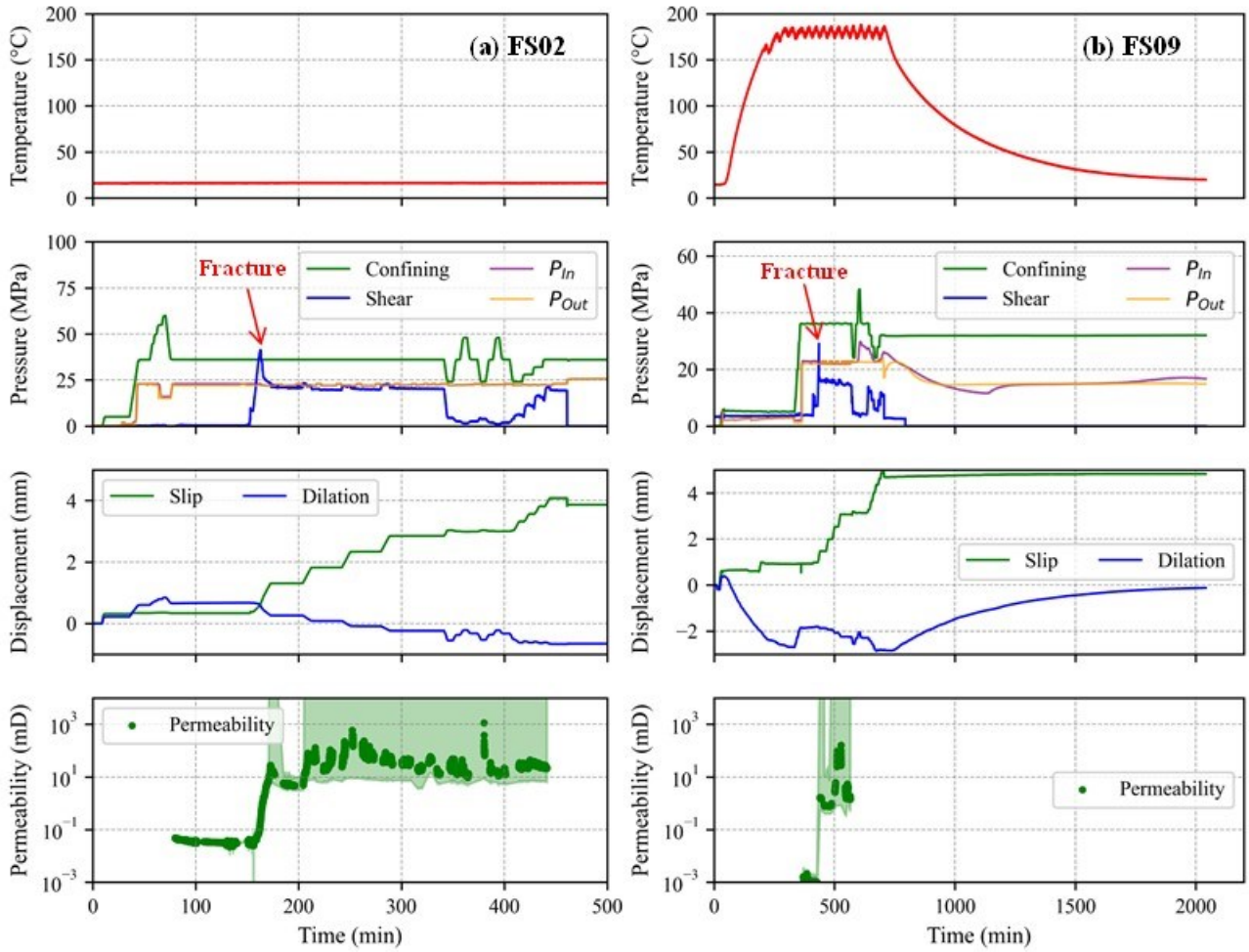


**Figure 2: Summary of the triaxial direct shear experiment result. The left column if for (a) FS02 specimen tested at room temperature and the right column is for (b) FS09 tested at temperature of 195 ± 15 °C. The first shows the test temperature, the second row shows the evolution of applied pressures and stress on the specimen, the third row shows the deformation of the specimen, and the fourth row shows the evolution of bulk permeability of the specimen. The light green shaded region is the uncertainty band of our permeability estimation. As the specimen sheared, the fracture provided a highly conductive flow path that reached the sensitivity limit of our system.**

Next, we investigate the impact of shear displacement on the permeability (Figure 3) to determine whether further shearing is likely to be effective for permeability enhancement at FORGE. In general, the bulk permeability of both specimens increased with increasing fracture displacement. In case of FS09 specimen, i.e. high temperature experiment, the bulk permeability increased from 1.2 mD at 0.5 mm fracture displacement to 52.8 mD when the cumulative fracture displacement was 2 mm. This is factor of 44 increase in permeability. The permeability enhanced by a factor of 28 for FS02 specimen, when the fracture displaced from 0.9 mm to 1.9 mm. Fractured FS02 specimen exhibited higher permeability than FS09 specimen at displacement of 2 mm. This could be because of the fracture roughness.

Although the permeability was enhanced by shear, it remained within mD range. Previous studies have shown that fracture permeabilities in the range of Darcy is required for economic EGS (KC et. al., 2024a). Proppants can be used to prop open the fracture to increase the fracture permeability for economic EGS (Jones et al., 2014; KC et al., 2024b; Norbeck and Latimer, 2023;). However, the long-term performance of various proppants under EGS condition is a topic of active research.

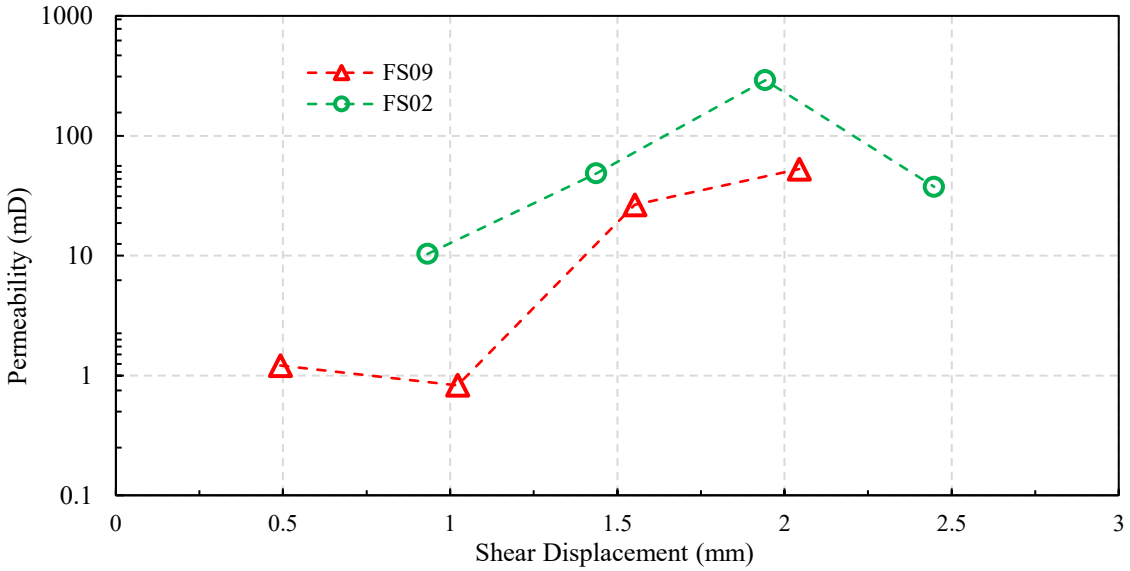


**Figure 3: Bulk permeability of the specimens during each shear displacement stage. In general, permeability increases with shear displacement, however it could decrease in some cases due to fines migrations and clogging of flow paths.**

### 3.2 FRACTURE DILATION AND COMPRESSIBILITY

Mechanical aperture of the fracture was measured using the radial LVDT sensor mounted across the specimen. The measured mechanical aperture can be plotted as the function of shear displacement (Figure 4) and effective normal stress (Figure 5) to estimate the dilation angle and compressibility of the fracture. These parameters are key inputs for field-scale multi-physics simulation of EGS. As seen in Figure 4, the mechanical aperture increases linearly with the shear displacement. Slope of the linear relationship in Figure 4 can be used to determine the dilation angle of the fracture on corresponding specimens (Barton et al., 1985).

The shear fracture on FS02 specimen tested at room temperature exhibited dilation angle of 22.7°, whereas the fracture on FS09 specimen resulted in the dilation angle of 10.2°. FS02 is a granitic sample. Our previous TDS experiments on granite, schist, amphibolite conducted at room temperature and similar effective stress conditions had dilation angles ranging from 0 to 38° (Li et al., 2021; Meng et al., 2022). However, at high temperature we observed the fracture dilation angle ranging from 0 to 10° (Frash et al., 2024; Iyare et al., 2024). Smaller dilation angles result in lower fracture permeability enhancement due to shearing. Therefore, these results indicate that permeability enhancement from shear will be less than we previously would have expected because of the elevated temperatures.

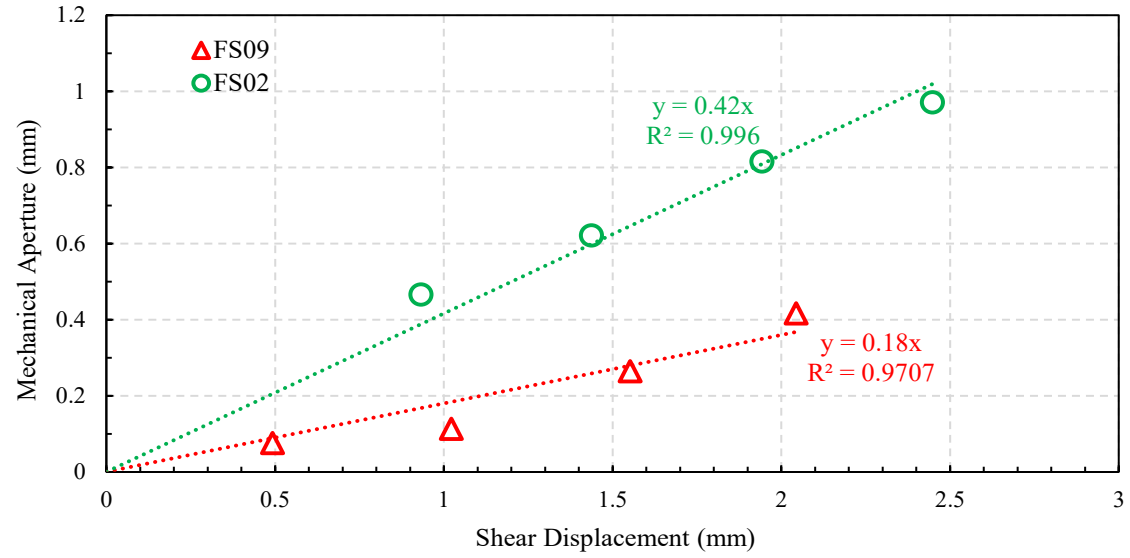


**Figure 4: Fracture shear dilation at FORGE conditions. Shearing under high temperature results in a lower dilation angle.**

To investigate the fracture compressibility, we used the mechanical aperture data during the loading stage, i.e. 24 MPa – 36 MPa – 48 MPa of confining stress cycling (Figure 5). It is worth noting that the stress cycling was done after the fracture was sheared by ~ 2 mm. Thus, the mechanical apertures are relatively large even at high effective stress. Fracture aperture decreased with increasing effective stress due to compaction of fracture. We elected to fit an exponential decay model to quantify the fracture compressibility (Li et al., 2021; Meng et al., 2022). These corresponding equations of fit are shown in Figure 5. The decay coefficients in these equations represents the fracture compressibility. The fracture compressibility of FS09 specimen is 3.5 times larger than that of FS02. The fracture compressibility observed for FS09 specimen is comparable to our previous experiments at similar temperature and stress conditions (Frash et al., 2024; Iyare et al., 2024), where fracture compressibility between $2.5e^{-8}$ to $3.2e^{-8}$ $Pa^{-1}$ was observed. Similarly, lower fracture compressibility in the range of $0.7e^{-8}$ to $2.0e^{-8}$ $Pa^{-1}$ was observed at low temperature TDS experiments (Meng et al., 2022) highlighting the impact of temperature on fracture compressibility. At higher temperatures, the rock strength decreases enhancing the asperities damage during shearing resulting in higher fracture compressibility. The exponential model presented in this study for rock at higher temperatures is scalable for reservoir simulation of EGS at FORGE.

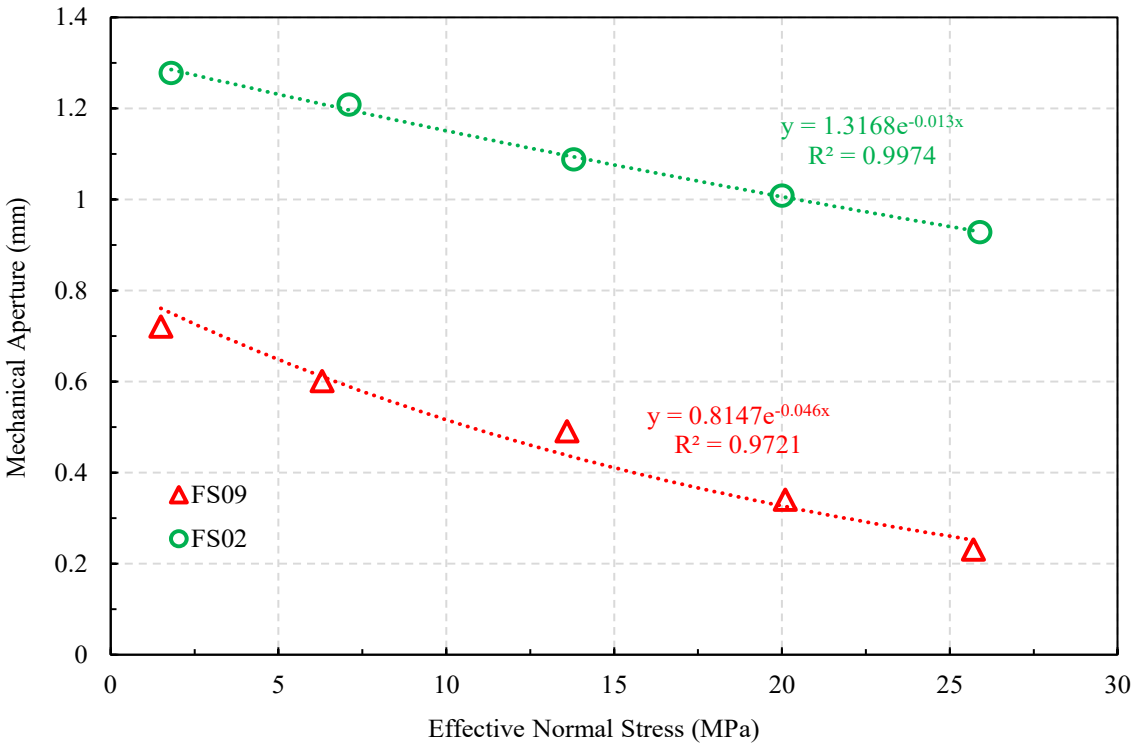


**Figure 5: Compressibility of the fractured specimens. Higher temperature correlates to higher compressibility.**

### 3.3 FRACTURE MECHANICAL PROPERTIES

Intact shear strength and fracture residual shear strength parameters, i.e., fracture cohesion and friction angle, were estimated for each sample (Figure 6). The intact shear strength of FS09 specimen was measured to be 29.1 MPa and that of specimen FS02 to be 48.8 MPa. This result is consistent with our previous findings, where we report the intact shear strength of granitic rock from 16A(78)-32 well at the FORGE to be in the range 38.1 to 47.1 MPa at in-situ temperature and pressure conditions (Iyare et al., 2024; Frash et al., 2024). The foliated specimens, similar to FS09 in the current study, exhibited the intact strength ranging between 25.0 to 30.8 MPa, due to presence of weak planes aligned along the shear direction. We sheared the fracture at different confining stress (i.e. Mohr-Coulomb shear stage in experimental procedure) to develop a Mohr-Coulomb-type failure envelope for each specimen (Figure 6). FS09 exhibited effective friction angle ($\emptyset'$) and effective cohesion ($c'$) of 33.8° and 5.82 MPa, respectively. FS02 specimen exhibited higher effective friction angle ($\emptyset'$) of 51.1° and effective cohesion of 4.82 MPa. These results are consistent with of previous TDS experiments which indicates that reservoir temperature at FORGE had minor impact on the intact and residual strength parameters of the rock at FORGE.

### 3.4 POST-TEST SPECIMENS

The TDS experiment resulted in a single diametral fracture across the length in both specimens. Fracture shearing created gouge particles due to crushing of fracture asperities as the fracture faces slid over each other. In case of FS02 specimen tested at room temperature, we observed large rock chips accompanied by fines on the post sheared fractures (Figure 7). In addition, the fracture surface was relatively rough. FS02 specimen contained pre-existing small-cracks which could have resulted in the large rock chips. On the other hand, FS09 specimen produced very little gouge particles (Figure 7). In our previous high temperature experiments on granitic specimen, we observed slickenside surface during shearing (Iyare et al., 2024). In the current study, the fracture surface on granitic rock at low temperature experiment did not exhibit any slickensides. However, we observed striation along the direction of shear on FS09 specimen at high temperature, indicating shearing of fracture at FORGE could result in slickenside fractures.

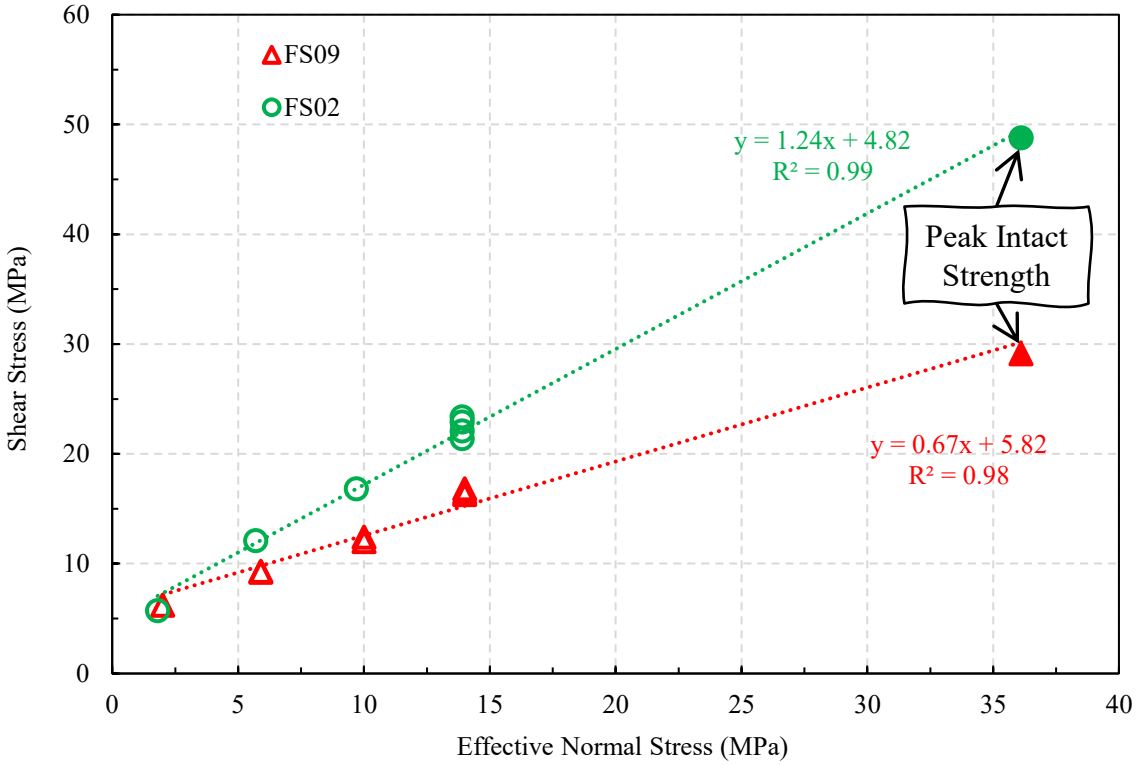


**Figure 6: Mohr-Coulomb strength estimates of the fracture based on the triaxial direct-shear test data. The filled markers represent corresponding intact shear strength. Since the Biot's coefficient of the ultra-low porosity rock is close to zero, the effective normal stress will be equal to the applied confining stress on the intact sample. Once the fracture is created, the Biot's coefficient will be equal to one, and the effective normal stress will be the difference between the confining and pore pressure. Shear stress can be directly measured using the load cell.**

We used temperature resistant silicone rubber to fill the gap in our L-shaped TDS platens. We observed the silicone rubber intruding into the pore-pressure ports as well as on the fracture surface. This rubber clogs the pore lines and fills the fracture surface, resulting in unreliable permeability data. In the current study, silicone rubber intruded the pore lines and fracture during the stress cycling stage when the confining pressure was increased to 48 MPa. This can be confirmed by the sudden increase in static inlet pore pressure (Figure 7). For future, experiments we intend to use only Viton rubber filler to mitigate this problem in high temperature and pressure experiments.

## 4. DATA AVAILABILITY AND FUTURE WORK

The measurements collected here will be made available on the Geothermal Data Repository (GDR). At the time of wiring this paper, we are still processing the accompanying geochemical influent and effluent data, so it is unfortunately not included here. When the complete dataset is submitted to GDR it will include timeseries information along with time-matched geochemistry data. We anticipate that the chemistry information will reveal exciting information about the slickenside shear fracture evolution because the elevated temperatures, flowing pore fluid, and shear mechanism appear to all be required for slickensides to form.

## 5. CONCLUSIONS

We presented the results from the Triaxial Direct Shear (TDS) experiments on granitic and gneissic core specimens retrieved from the EGS reservoir at the FORGE site. The experiment on granitic core specimen was conducted at room temperature, whereas the gneissic specimen was tested at temperature of 195 ± 15 °C. Based on the experimental results, following conclusions can be drawn:

1. New fractures can enhance the permeability by 4 to 5 orders of magnitude, whereas subsequent shearing of the fracture only resulted in an order of magnitude increase in permeability. Therefore, EGS stimulation should target to create new fractures rather than shear stimulation of pre-existing fractures.
2. Shear at high temperature exhibits lower than expected dilation angle (0 to 10° dilation at 195 °C) compared to lower temperature experiments (0 to 38° dilation at 23 °C) on similar rock materials at similar stress conditions.
3. The granitic rock at FORGE exhibited higher intact strength and higher residual shear strength when compared to the gneissic rock with foliations.
4. Fractures at higher temperature have higher compressibility, i.e., $2.5e^{-8}$ to $4.6e^{-8}$ $Pa^{-1}$, compared to our current and prior results at low temperature where the compressibility ranged between $0.7e^{-8}$ to $2.0e^{-8}$ $Pa^{-1}$ were observed.
5. Injection induced shear stimulation of fractures at FORGE conditions appears to induce slickensided fracture surfaces, which indicates that shear stimulation could be less effective than previously expected.

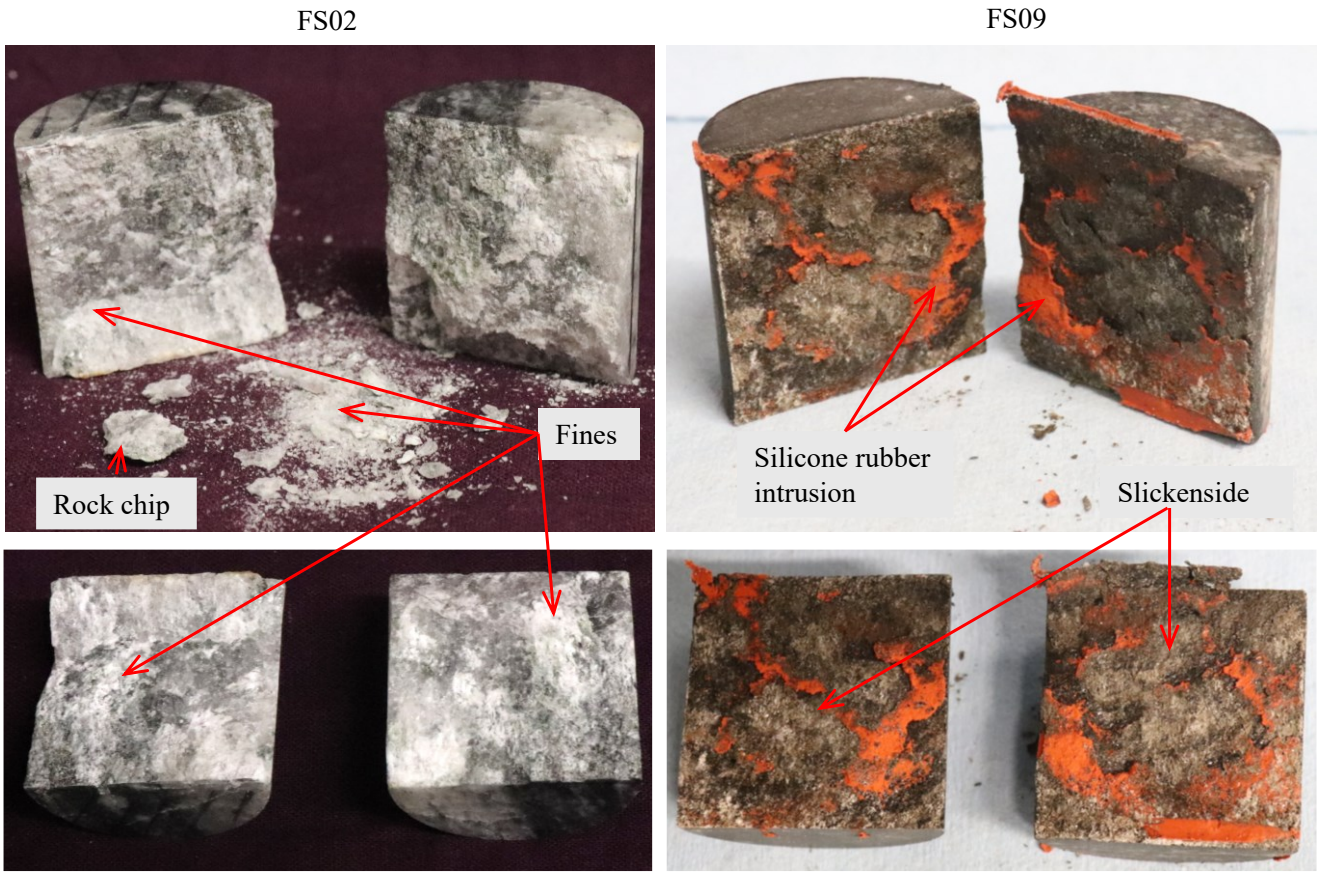


**Figure 7: Post-sheared specimens showing the single-stranded diametric fractures and gouge particles that were formed by shear. In the high temperature experiment, a slickenside surface was evident.**

**ACKNOWLEDGEMENTS**

This work was funded by Department of Energy (DOE) Basic Energy Sciences under FWP LANLE3W1. Support was also provided by Geothermal Technologies Office (GTO) Frontier Observatory for Research in Geothermal Energy (FORGE) via grant DE-EE0007080 with Lawrence Livermore National Laboratory. The unlimited public release number for this paper is LA-UR-25-20548.

**REFERENCES**

Allis, R. G., & Larsen, G. Roosevelt Hot Springs Geothermal field, Utah–reservoir response after more than 25 years of power production. In *Proceedings of the 37th Workshop on Geothermal Reservoir Engineering*. *Stanford University*. *Stanford, CA,* (2012).

Augustine, C. R., Ho, J. L., & Blair, N. J. GeoVision analysis supporting task force report: Electric sector potential to penetration. *National Renewable Energy Laboratory, NREL/TP-6A20-71833,* (2019).

Barton, N., Bandis, S. C., & Bakhtar, K. Strength, deformation and conductivity coupling of rock joints. In *International Journal of Rock Mechanics and Mining Sciences & Geomechanics Abstracts*, 22(3), 121-140, (1985).

Brown, D. W., Duchane, D. V., Heiken, G., & Hriscu, V. T. Mining the earth's heat: hot dry rock geothermal energy. *Springer Science & Business Media.* (2012).

Cyrq Energy. Thermo Geothermal Power Plant. https://cyrqenergy.com/energy-plant-locations/#minersville-ut (2025). <last accessed on Jan. 20, 2025).

Dobson, P. F., Kneafsey, T. J., Nakagawa, S., Sonnenthal, E. L., Voltolini, M., Smith, J. T., & Borglin, S. E. Fracture sustainability in Enhanced Geothermal Systems: Experimental and modeling constraints. *Journal of Energy Resources Technology*, *143*,10, 100901, (2021).

Frash, L. P., Iyare, U. C., KC, B., Meng, M., Smith, M., & Kroll, K. High Temperature Triaxial Direct-Shear Testing for FORGE and Field Scale Implications. In *ARMA US Rock Mechanics/Geomechanics Symposium, Golden, CO.* (p. D042S059R005), (2024).

Iyare, U. C., Frash, L. P., K C, Bijay, Meng, M., Kroll, K., Smith, M. M., ... & Carey, J. W. Measurements of Thermo-Hydro-Mechanical-Chemical Coupling in Granite Shear Fractures at FORGE using the Triaxial Direct-Shear Test Method. In *Proceedings of the 49th Workshop on Geothermal Reservoir Engineering*. *Stanford University*. *Stanford, CA,* (2024).

Jones, C. G., Simmons, S. F., & Moore, J. N. Proppant behavior under simulated geothermal reservoir conditions. In *Proceedings of 39th workshop on geothermal reservoir engineering, Stanford University, Stanford, CA,* (2014).

Jones, C., Simmons, S., & Moore, J. Geology of the Utah Frontier Observatory for Research in Geothermal Energy (FORGE) Enhanced Geothermal System (EGS) Site. *Geothermics*, *122*, 103054, (2024).

KC, B., Frash, L. P., & Ahmmed, B. Minimum Propped Fracture Permeability for Economic Multi-stage Enhanced Geothermal Systems. In *49th Workshop on Geothermal Reservoir Engineering, Stanford University*. *Stanford, CA,* (2024a).

KC, B., Ghazanfari, E., McLennan, J., Frash, L. P., & Meng, M. Evaluation of sintered bauxite proppant for binary enhanced geothermal systems. *Geomechanics and Geophysics for Geo-Energy and Geo-Resources*, *10*(1), 21, (2024b).

Kneafsey, T., Neupane, G., Blankenship, D., Dobson, P., White, M., Morris, J., ... & EGS Collab Team. Scientific Findings to Engineering Realities: Coordination across Collab teams and making the connection to FORGE. *Lawrence Berkeley National Laboratory*. *Report #: LBNL-2001564,* (2021).

Li, W., Frash, L. P., Welch, N. J., Carey, J. W., Meng, M., & Wigand, M. Stress-dependent fracture permeability measurements and implications for shale gas production. *Fuel*, *290*, 119984. (2021).

McLennan, J., England, K., Rose, P., Moore, J., & Barker, B. Stimulation of a high-temperature granitic reservoir at the Utah FORGE Site. In *SPE Hydraulic Fracturing Technology Conference and Exhibition, The Woodlands, TX* (p. D031S008R001). SPE. (2023)

Meng, M., Frash, L. P., Li, W., Welch, N. J., Carey, J. W., Morris, J., ... & Kneafsey, T. Hydro-mechanical measurements of sheared crystalline rock fractures with applications for EGS Collab Experiments 1 and 2. *Journal of Geophysical Research: Solid Earth*, *127*(2), e2021JB023000. (2022).

Moore, J., McLennan, J., Pankow, K., Finnila, A., Dyer, B., Karvounis, D., ... & Damjanac, B. Current activities at the Utah frontier observatory for research in geothermal energy (FORGE): A laboratory for characterizing, creating and sustaining enhanced geothermal systems. In *ARMA US Rock Mechanics/Geomechanics Symposium, Atalanta, GA* (pp. ARMA-2023). ARMA. (2023).

Moore, J., McLennan, J., Pankow, K., Simmons, S., Podgorney, R., Wannamaker, P., ... & Xing, P. The Utah Frontier Observatory for Research in Geothermal Energy (FORGE): A Laboratory for characterizing, creating and sustaining enhanced geothermal systems. In *Proceedings of the 45th Workshop on Geothermal Reservoir Engineering*. *Stanford University*. *Stanford, CA,* (2020).

Norbeck, J. H., Gradl, C., & Latimer, T. Deployment of Enhanced Geothermal System technology leads to rapid cost reductions and performance improvements. Pre-print at https://doi.org/10.31223/X5VH8C (2024).

Norbeck, J. & Latimer, T. Commercial-scale demonstration of a first-of-a-kind enhanced geothermal system. Preprint at https://doi.org/10.31223/X52X0B (2023).

Tester, J. W., Anderson, B. J., Batchelor, A. S., Blackwell, D. D., DiPippo, R., Drake, E. M., ... & Petty, S. The Future of Geothermal Energy. *Massachusetts Institute of Technology,* (2006).

Witherspoon, P. A., Wang, J. S., Iwai, K., & Gale, J. E. Validity of cubic law for fluid flow in a deformable rock fracture. *Water resources research*, *16*(6), 1016-1024, (1980).

Xing, P., McLennan, J., & Moore, J. In-situ Stress Measurements at the Utah Frontier Observatory for Research in Geothermal Energy (FORGE) site. *Energies*, *13*(21), 5842, (2020).